ISBN: 978-3-95450-241-7 ISSN: 2673-5350 doi:10.18429/JACoW-IBIC2022-WEP17

SECONDARY ELECTRON EMISSION (SEM) GRID FOR THE FAIR PROTON LINAC

J. Herranz, Proactive R&D, Sabadell, Spain
T. Sieber, P. Forck, GSI, Darmstadt, Germany
I. Bustinduy, A. Rodriguez Paramo, ESS Bilbao, Zamudio, Spain
A. Navarro Fernandez, CERN, Geneva, Switzerland

Abstract

New SEM-Grid has been developed for FAIR Proton Linac, the instrument consists of 2 harps fixed together in an orthogonal way. This SEM-Grid will provide higher resolution and accuracy measurements as each HARP consists of 64 tungsten wires 100 µm in diameter and 0.5 mm pitch. Each wire is fixed to a ceramic PCB with an innovative dynamic stretching system, this system assures wire straightness under typical thermal expansion due to beam heat deposition. Simulation calculations of electric field distribution have been performed, three main parameters have been optimized, wires distribution, quantity of polarization electrodes and distance between electrodes and wires. The design and production of the SEM-Grid has been performed by the company Proactive R&D that has counted on the expertise of ESS-Bilbao to define safe operation limits and signal estimation by means of a code developed specifically for this type of calculations. Preliminary validations of the first prototypes have shown excellent mechanical and electrical behaviour. After the successful beam test validations performed in June 2022, final series of the SEM-Grid will be produced to be installed on FAIR proton LINAC.

FAIR PROJECT INTRODUCTION

The FAIR [1] facility at GSI will provide antiproton and ion beams of worldwide unique intensity and quality for fundamental physics research.

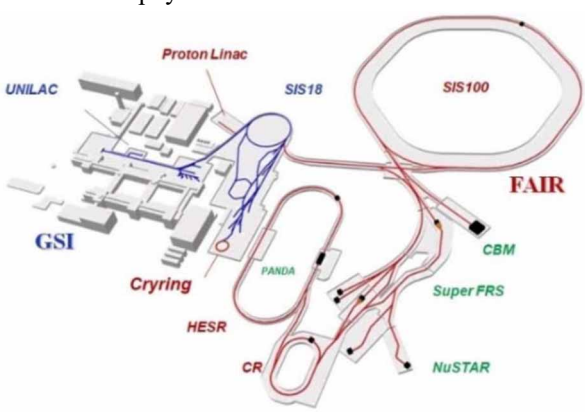

Figure 1: Layout of the FAIR facility.

The accelerator facility of FAIR, shown in Fig. 1, will include three linear accelerators, the existing UNILAC (for which a refurbishing program is currently on the way), a superconducting cw-Linac, designed mainly for intermediate energy experiments [2], and the new proton Linac (pLinac) [3]. The UNILAC and pLinac will be the main injectors of SIS18, which will in turn be an injector for SIS100, the central accelerator component of FAIR.

The pLinac consists of a novel so called 'Ladder' RFQ [4] followed by two ~10 m sections of Cross Bar H-drifttube accelerator (CH) structures [5]. The first section includes six CH modules, which are pairwise rf-coupled (Coupled CH or CCH). The second section consists of three separate modules, each connected to its own klystron. The pLinac will deliver a current up to 70 mA with a macropulse length of 35 µs (at max. 4 Hz) and a typical bunch length of 100 ps. The design energy is 68 MeV. Figure 2 shows a schematic of the pLinac and its beam instrumentation.

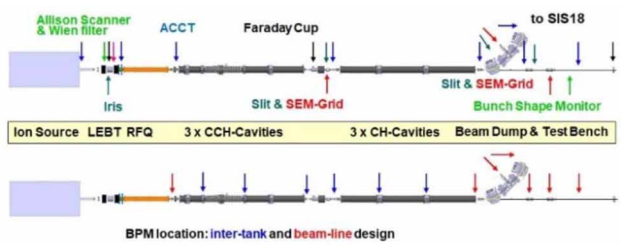

Figure 2: Schematic of the FAIR pLinac, side view, showing the location of diagnostics (upper) and BPMs, divided in cavity (inter-tank) and beamline BPMs (lower).

The overall diagnostics concept and layout of pLinac has been described in various reports, e.g. [6]. Because of the compact structure of the two CH sections, diagnostics (except BPMs) will be concentrated in the LEBT, in the MEBT behind the RFQ and in a diagnostics/rebuncher (so called SD) section between the CCH and CH parts of the pLinac. Additional beam diagnostics elements are placed in the transfer line to SIS18 as well as in a straight line to the beam dump.

Special care has been taken for the design of the SEM Grids. We expect a 1 σ beam radius of 1.5 mm in the "worst case", therefore the wire pitch cannot be larger than 0.5 mm to obtain realistic profiles. Moreover, a stretching mechanism is required to compensate for thermal expansion, even if the grids are operated in a "grid protection mode" at reduced duty cycle. Any kind of plating on the tungsten wires must be considered carefully because of possible melting and agglutination during irradiation.

SEM GRID DESIGN

The working principle of SEM grids is based on secondary electrons, which are released from the grid wires up on ion beam impact. The resulting current distribution

ISBN: 978-3-95450-241-7 ISSN: 2673-5350 doi:10.18429/JACoW-IBIC2022-WEP17

on an array of wires represents the beam profile in a given direction [7]. While grids cover both directions, harps cover only one coordinate axis. Due to the smaller size of the pLinac beam as compared to the UNILAC heavy ion beam, the traditional grid design of GSI only can be used for the LEBT section. The LEBT SEM grid is made of 64 wires with 2.0 mm spacing for each plane. It is designed in a classical way, consisting of a frame with spring holders for each wire.

The grids for the Linac section (SD-section, inflection and dump), designed by PROACTIVE R&D company in collaboration with GSI, have a smaller wire spacing of 0.5 mm. The active area is 32 × 32 mm^2 corresponding to 64 wires for each plane. At the inflection and in the rebuncher (SD) section a grid for both transverse directions mounted on a pneumatic drive. However, at the dump and additionally in the SD section separate harps for the horizontal and vertical profiles are mounted on two stepping motor drives to allow for transverse emittance measurements in connection with two upstream slits. Table 1 shows the relevant parameters.

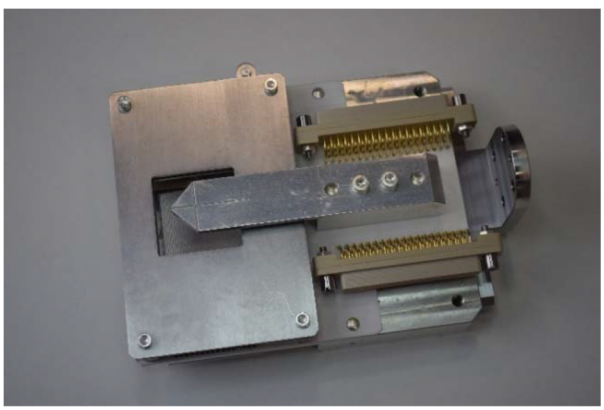

Figure 3: SEM harp by PROACTIVE R&D. The grid consists of two harps rotated by 90°, area 32 mm × 32 mm with diamond shaped cleaning electrode, 64 wires per harp, wire pitch 0.5 mm, thickness 100 µm.

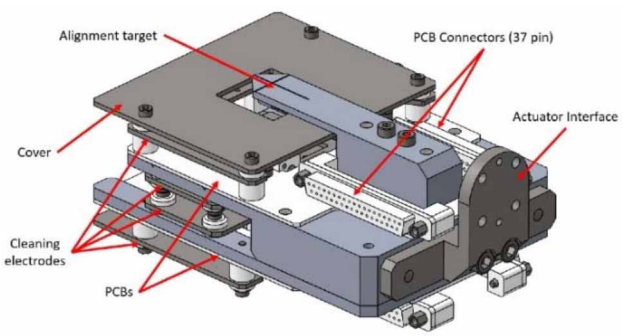

Figure 4: SEM grid design by PROACTIVE R&D.

The mechanical design of the grid can be seen in Figs. 3 and 4. The structure is based on a PCB to which the wires are soldered on one side. On the other side, a specially designed stretching system is used to keep wires under tension during irradiation.

Besides high resolution and a compact design, special care has been taken for the field distribution due to the cleaning electrodes. These electrodes are kept at a positive

Table 1: Parameters of pLinac and SEM Grids

No. of Grids / Harps	2 / 4
No. of wires Grid / Harp	2 × 64 / 1 × 64
Wire pitch / diameter	0.5 mm / 100 µm
Wire material	Tungsten (gold plated)
Detection area	32 × 32 mm^2
Vacuum requirement	$5 \cdot 10^{-9}$ mbar (no bakeout)
Max. beam current	70 mA
Pulse duration	10 – 100 µs
Repetition rate	1 – 4 Hz
Max. beam energy	68 MeV
Normal / max. grid temp.	2000 K / 3000 K

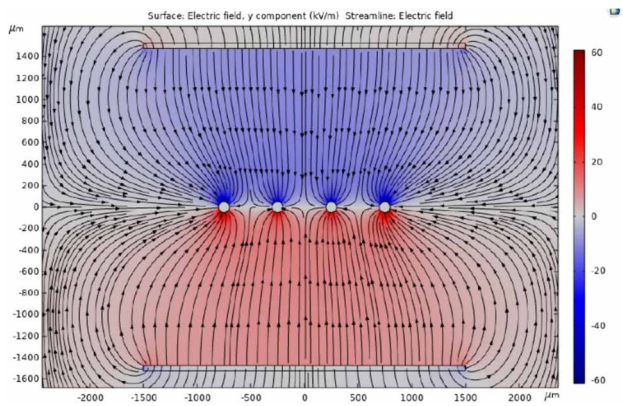

Figure 5: Field distribution calculated for co-planar wires. The diamond shaped cleaning electrodes are located at top and bottom respectively.

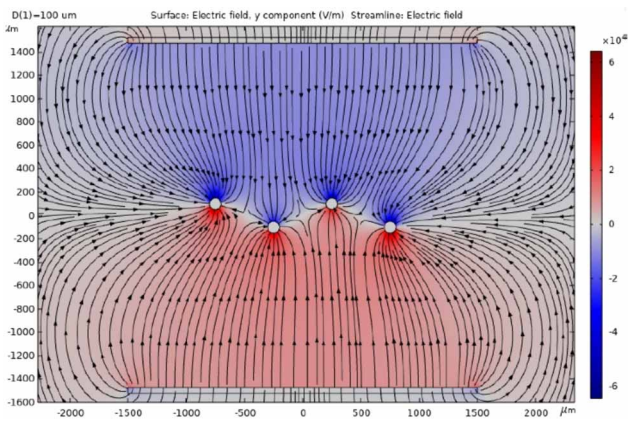

Figure 6: Field distribution with alternating wire positions. The diamond shaped cleaning electrodes are located at top and bottom respectively.

potential to extract the secondary electrons and thus prevent them from being captured by neighboring wires, which would deteriorate the measurement. The electric field distribution obtained with a parallel oriented diamond shaped electrode configuration is shown in Figs. 5 and 6. The potential required for the cleaning electrodes has been estimated to be ~200 V. As can be seen, the electric field vanishes in the plane where the four (representative) wires

ISBN: 978-3-95450-241-7 ISSN: 2673-5350 doi:10.18429/JACoW-IBIC2022-WEP17

are located. Consequently, a secondary electron generated at one of the wires and directed towards another one cannot be properly deterred from reaching it. This issue could generate unwanted crosstalk between the wires.

In order to solve this issue, a new, non-planar disposition of the wires has been studied. The electric field distribution of this new design is also shown in Figs. 5 and 6. As can be seen, with this new wire distribution the vanishing electric field plane is avoided, instead a rather sinusoidal shaped surface is observed on which the electric field vanishes. The electric field along a line joining two consecutive wires proves to be strongly repelling for electrons towards the ends of this line. A wire displacement of only 0.2 mm should provide a significant background reduction.

SEM GRID ACCEPTANCE TEST

The test of two prototype y-harps (gold coated / uncoated tungsten wires) was performed in two steps, in a first campaign a low intensity proton beam was used to prove the correct function of the harp in connection with the POLAND+ CSA electronics (proton beam parameters, see BPM section [8]). A second experimental campaign was performed with a high intensity Ar beam to check the wire stretching system, the upper limit of acceptable energy deposition and the actual heat load in comparison to simulations. The beamtime started with gold plated wires, later we switched to a harp with regular tungsten wires. We used an Ar_{10+} beam at 8.6 MeV/u, intensities 20 µA to 1.5 mA, pulse length 40 µs to 200 µs, repetition rate 1 Hz. In parallel to the measurements, simulations for wire heating were done with the pyTT code [9], predicting the wire temperature at the various measurements.

We checked the effect of the voltage on the diamond shaped cleaning electrode (extraction of secondary electrons to reduce wire cross-talk) while varying beam parameters. Figure 7 shows the voltage dependence of the integrated number of particles for two different spot sizes.

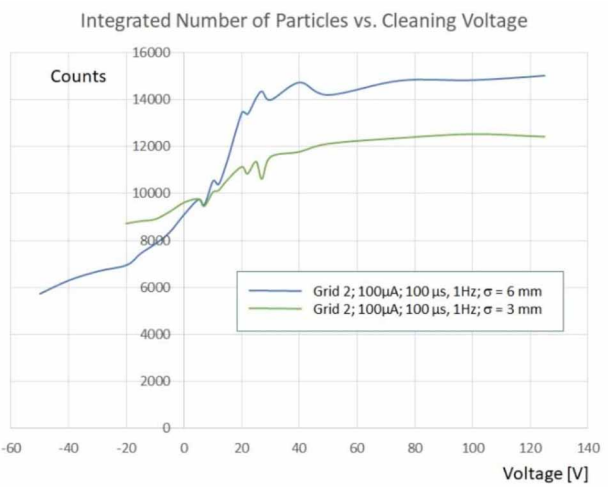

Figure 7: Number of particles, as a function of cleaning voltage. Sigma values indicate the beam size assuming Gaussian distribution in the calculations.

If the maximum current on the grid wires (maximum total counts) is taken as a criterion for optimum voltage, there is obviously not much effect from the cleaning electrode above ~40 V, which significantly reduces the effort for electrical connections. With proton beam, the saturation voltage was even smaller (<10 V). A comparison of the two curves in Fig. 5 shows that the number of counts is reduced most likely due to geometrical aspects at the smaller number of wires, while an effect on the slope of the curves cannot be observed (at given accuracy), which is a strong hint for a homogeneous field distribution as result of our electrode geometry optimization.

At inspection the gold plated grid showed no damage, even after heating to (theoretically) >2500 K. From this we concluded, that the wire temperature might have been overestimated in our calculations. Beam parameters (such as beam size, beam intensity, pulse length, etc.) and material properties (such as emissivity) are crucial for accurate thermal modeling. Big uncertainties on beam spot size and the emissivity of the material yielded too large uncertainties in the predicted temperatures. In an ideal case, temperature calibration measurements should be performed, which could not be done for several reasons. Thus, a systematic approach has been adopted to prove the suitability of the SEM grids. The harp was irradiated in the regular UNILAC 'grid protection mode', which at a spot size of σ = 3 mm an intensity of 500 µA and duration of 40 µs corresponds to a (calculated) temperature of ~2800 K. Starting from this point, the intensity and the pulse length were stepwise increased to 1.4 mA, 40 µs, which lead after a final step to 70 µs to destruction of some wires (T_{calc} = ~4200 K). The reasons for the strong increase of the current in Fig. 8, besides the position of the broken wires, is not clear. Several aspects contribute to the dynamic development of the profile, like time constant of the electronics and intensity variation during macro pulse.

To what extent thermionic emission plays a role has to be investigated. Analysis of the results and adjustment of our theoretical model is ongoing.

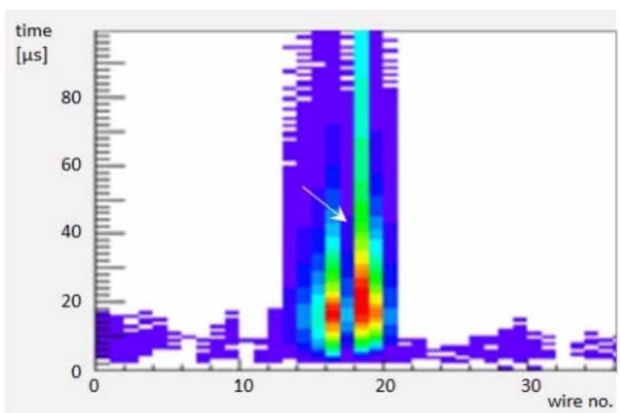

Figure 8: Development of the beam profile during one 70 µs macro pulse at destruction of one wire. Total span 100 µs, time slice 1 µs.

ISBN: 978-3-95450-241-7 ISSN: 2673-5350 doi:10.18429/JACoW-IBIC2022-WEP17

REFERENCES

[1] O. K. Kester, "Status of the FAIR Facility", in *Proc. IPAC'13*, Shanghai, China, May 2013, paper TUXB101, pp. 1085-1089.

[2] M. Miski-Oglu *et al.*, "Beam Commissioning of the Demonstrator Setup for the superconducting cw HMI/GSI Linac", *J. Phys.: Conf. Ser.*, vol. 1350, p. 012089, 2019. doi:10.1088/1742-6596/1350/1/012089

[3] L. Groening *et al.*, "Status of the FAIR 70 MeV Proton Linac", in *Proc. LINAC'12*, Tel Aviv, Israel, Sep. 2012, paper THPB034, pp. 927-929.

[4] R. M. Brodhage, A. Almomani, and U. Ratzinger, "Design Study of a High Frequency Proton Ladder RFQ", in *Proc. IPAC'13*, Shanghai, China, May 2013, paper THPWO014, pp. 3788-3790.

[5] G. Clemente *et al.*, "Development of room temperature crossbar-*H*-mode cavities", *Phys. Rev. ST Accel. Beams*, vol. 14, p. 110101, 2011. doi:10.1103/PhysRevSTAB.14.110101

[6] T. Sieber *et al.*, "Beam Diagnostics Layout for the FAIR Proton Linac", in *Proc. LINAC'14*, Geneva, Switzerland, Aug.-Sep. 2014, paper THPP063, pp. 998-1000.

[7] P. Forck, "Lecture Notes on Beam Instrumentation and Diagnostics", presented at Joint University Accelerator School (JUAS), Jan. 2011.

[8] M. Witthaus *et al.*, "SEM-GRID Prototype Electronics using Charge-Frequency-Converters", in *Proc. DIPAC'11*, Hamburg, Germany, May 2011, paper MOPD55, pp. 176-178.

[9] A. Navarro Fernandez, F. Roncarolo, and M. Sapinski, "Development of a Thermal Response Model for Wire Grid Profile Monitors and Benchmarking to CERN LINAC4 Experiments", in *Proc. IBIC'20*, Santos, Brazil, Sep. 2020, pp. 82-85. doi:10.18429/JACoW-IBIC2020-TUPP35